



Short communication

Diffusion tensor imaging for spatially-resolved characterization of muscle fiber structure in seafood

Kathryn E. Anderssen^{a,*}, Mathias Kranz^{b,c}, Shaheen Syed^a, Svein Kristian Stormo^a^a Department of Seafood Industry, Nofima AS, P.O. Box 6122, 9291 Tromsø, Norway^b PET Imaging Center Tromsø, University Hospital North-Norway (UNN), 9009 Tromsø, Norway^c Nuclear Medicine and Radiation Biology Research Group, The Arctic University of Norway, UiT, 9009 Tromsø, Norway

ARTICLE INFO

Keywords:

Magnetic resonance imaging
Diffusion tensor imaging
Tissue structure
Fish

ABSTRACT

The fiber structure of tissue in meat and seafood has a significant impact on their perceived quality. However, quantifiable description of muscle structure is challenging. We investigate diffusion tensor imaging (DTI) magnetic resonance imaging (MRI) as a method to quantitatively describe tissue structure. DTI measures the anisotropy of water molecule diffusion within muscle fibers. A pilot study evaluated three different cod loin samples: one of high-quality, one of medium-quality, and one of poor-quality. DTI parameters such as fractional anisotropy, axial diffusion and radial diffusion showed clear differences between the sample qualities. Changes in the DTI metrics consistent with freezing and thawing damage to the tissue were observed. The DTI maps were compared to T₂-weighted images and DTI detected significant details that were not visible in T₂-weighted images. Overall, these results indicate that DTI is a promising method for spatially-resolved characterization of tissue structure in seafood and meat.

1. Introduction

Characterizing the quality of meat and seafood products is a challenge. Sensory methods are typically considered the gold standard for determining whether a sample has the properties associated with a high or low-quality product. However, sensory evaluation has drawbacks in that the results are subjective, limited to a small number of samples, and cannot be used for screening industrially (Hyldig & Green-Petersen, 2008). For meat and seafood, muscle fiber structure has a significant influence on the perceived quality. Previous research indicates that fiber density is positively correlated with sensory properties such as chewiness, firmness, mouth-feel and dryness (Johnston et al., 2000). Therefore, a method to quantitatively characterize muscle structure would provide a useful metric for evaluating sample quality. Unfortunately, current methods to provide information on microstructure of meat and seafood are limited. Light microscopy of the tissue can provide information on fiber size, density, and structure, but it is only available in two-dimensions at one time, is limited to small subsections, and destroys samples such that they cannot be used for further investigations (Kalab et al., 1995).

Magnetic resonance imaging (MRI) is a method that has been used to provide spatial and structural characterization of meat and seafood

samples. MRI has been used to characterize tissue changes due to processing such as brining (Aursand et al., 2009; Erikson et al., 2004; Gudjonsdottir et al., 2015; Vestergaard et al., 2005) or freezing and thawing (Howell et al., 1996; Nott et al., 1999). However, these studies tended to be qualitative. Previous work applied machine learning and T₂-weighted MRI images as a method to quantify damaged tissue associated with freezing and thawing (Anderssen et al., 2021). Recent research indicates that numerous effects can influence the T₂ relaxation in tissue and changes to the fiber structure may not dominate other sources of relaxation (Anderssen & McCarney, 2022). Therefore, in order to focus on changes to the physical structure of the tissue during processing, we propose that diffusion tensor imaging (DTI) is a more suitable method. DTI is a technique originally developed for investigation of brain disease and damage (Basser, 1995). While the method is widely used in medical studies, its application beyond the medical domain has been limited. In this article, we perform a small pilot study to investigate its potential to identify changes and damage to tissue due to processing.

Pulsed-field gradient nuclear magnetic resonance (NMR) is a well-established technique for measuring the self-diffusion coefficients of molecules (Callaghan, 2011). In the presence of an applied field gradient, molecules will have their NMR signal attenuated

* Corresponding author.

E-mail address: kate.anderssen@nofima.no (K.E. Anderssen).<https://doi.org/10.1016/j.foodchem.2022.132099>

Received 13 September 2021; Received in revised form 5 January 2022; Accepted 5 January 2022

Available online 8 January 2022

0308-8146/© 2022 The Authors. Published by Elsevier Ltd. This is an open access article under the CC BY license (<http://creativecommons.org/licenses/by/4.0/>).

proportionally to how far they have moved during the mixing time. This effect is described by the equation:

$$S = S_0 e^{-D\gamma^2 \delta^2 g^2 (\Delta - \delta/3)} \quad (1)$$

where S_0 is the signal observed in the absence of a gradient, D is the diffusion coefficient of the molecule, γ is the gyromagnetic ratio of the observed nucleus, δ is the applied gradient duration, g is the gradient amplitude, and Δ is the diffusion time. Equation (1) is sometime simplified such that all the pulsed field gradient parameters are combined into a single variable, b :

$$S = S_0 e^{-bD} \quad (2)$$

where $b = \gamma^2 \delta^2 g^2 (\Delta - \delta/3)$. When water molecules are placed in a porous matrix like tissue, the free diffusion of the water molecules is limited by the presence of barriers. Depending on the structure of the tissue, the diffusion may be more limited in some directions than others. For example, many cells like muscle or nerve cells are very long and thin. Water molecules are able to freely diffuse a much longer distance along the long axis of the cell than perpendicular to it. Diffusion tensor imaging measures the diffusion coefficient in multiple dimensions in a three-dimensional sample, which is described by the equation:

$$D = \begin{pmatrix} D_{xx} & D_{yx} & D_{zx} \\ D_{xy} & D_{yy} & D_{zy} \\ D_{xz} & D_{yz} & D_{zz} \end{pmatrix} \quad (3)$$

From this, a diffusion tensor is calculated in each voxel, which describes the diffusion of water in that location of the sample. More detailed treatment of the mathematics of the measurement is beyond the scope of this paper but can be found elsewhere (Le Bihan et al., 2001). Several parameters are associated with the diffusion tensor, shown Fig. 1.

The fractional anisotropy (FA) describes the extent of anisotropic movement and is measured on a scale from 0 to 1, with a higher score indicating a greater degree of anisotropic movement. The radial diffusivity (RD) describes the diffusion along the short axis of the diffusion tensor. The axial diffusivity (AD) describes the diffusivity along the long axis of the diffusion tensor. Solving for equations 1–3 when the DTI data is analyzed produces a 2D map of these values for each image slice in a sample. Therefore, by using DTI, it is possible to focus on structural changes in the samples, as it is sensitive to the physical form of the sample, as opposed to methods like T_2 -weighting, which are also sensitive to the chemical composition of the tissue. The aim of this study was to evaluate whether the DTI metrics (FA, AD and RD) could characterize the differences in muscle structure between samples of high, medium, and poor quality.

2. Materials and methods

2.1. Samples

Atlantic cod fish (*Gadus morhua*) were received from the Tromsø

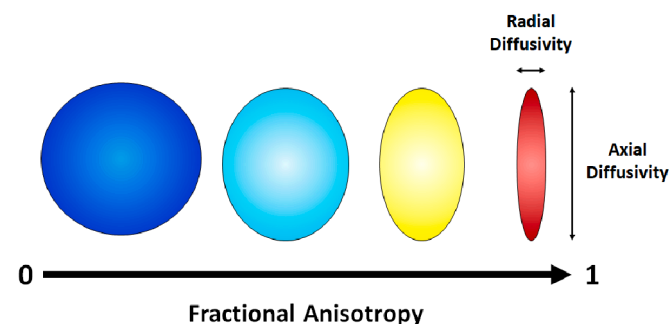


Fig. 1. Explanation of diffusion tensor imaging metrics.

Aquaculture Research Station (Kvaløya, Norway). The fish were killed by a blow to the head and immediately gutted. They were bled for 30 mins, iced and transported to Nofima (Tromsø, Norway), where they were kept on ice for 4 days to ensure that the fish were out of rigor prior to filleting. Three samples were investigated, each taken from the loin portion of the fillets. One sample (210.7 g) was measured immediately after filleting. The other two samples had undergone three years of storage at -22°C (183.4 g) and -35°C (156.3 g) respectively. These two samples are taken from another, ongoing study on the effect of temperature on long-term storage and the main results from that study will be published elsewhere. Even if -18°C is considered to be the standard deep-freezing temperature limit, most cold storage depots keep a stable temperature of -22°C . This ensures temperatures at -18°C or below to buffer for cargo flux in and out of the depot and to have some capacity to lower the temperature of goods. However, long-term storage at this temperature is deleterious to sample quality and other researchers have found that effective long-term storage of fish can be achieved from -35°C (Tolstorebrov et al., 2016). As such, the three samples were selected for use here because of the obvious quality differences between them. The fresh sample is considered a high-quality sample, the sample stored at -35°C a medium-quality sample, and the sample stored at -22°C a poor-quality sample.

2.2. Cod sample quality evaluation

Thaw loss was measured from the two samples. Liquid loss was collected directly from the vacuum packages. The vacuum-packed samples containing fish muscle and expelled liquid were opened after thawing from frozen storage. Loins were then repackaged for MRI imaging. Liquid loss was determined according to the formula:

$$LL = \frac{m_0 - m_L}{m_0} \times 100\%$$

where LL is liquid loss, m_0 is the initial weight of the loin, and m_L is the weight of the loin after thawing. In addition, thaw loss and a consumer test (8 tasters) to evaluate sensory quality were performed on samples that had experienced the same storage condition as the two samples measured in this study. Samples were rated on a scale of 1 to 5, with 5 being the highest quality mark. These samples were not imaged due to concerns the imaging process at ambient temperature could affect their sensory properties.

2.3. MRI acquisition and data processing

MRI images of the fresh and thawed samples were acquired using a preclinical 7 Tesla MR Scanner (MRS*DRYMAG, MR solutions, Guildford, UK) with a rat quadrature bird cage coil (\varnothing 65 mm, length 70 mm). T_2 -weighted images were taken in the axial direction using a Fast Spin Echo sequence. Repetition time (TR) was 8 s, echo time (TE) was 45 ms, slice thickness was 1 mm and the number of slices was 54. Field of View (FOV) was 60 mm and each image was 256×256 pixels, giving a resolution of approximately $240 \mu\text{m}$. Total measurement time was approximately 8 min. Diffusion tensor images were taken using a Fast Spin Echo sequence. TR was 6 s, TE was 35 ms and diffusion was measured in 10 sampling directions. The b value was 800 s/mm^2 , in-plane resolution is $500 \mu\text{m}$ by $500 \mu\text{m}$, slice thickness was 1 mm and number of slices was 60. Total measurement time was approximately 2 h. Diffusion tensor images were processed using DSI studio (Yeh, 2021). Reconstruction of the fiber tractography was performed according to the methods laid out in Yeh et al. (2013).

2.4. Statistical analysis of magnetic resonance images

Statistical analysis was performed on all the FA, RD and AD images from each sample in Python (Python Software Foundation, Delaware, USA). For each sample, the DTI metrics of each pixel were compiled

from every image slice into a single matrix. Note, as the values of FA, RD and AD outside the sample in the image are zero, these values were discarded for analysis. The distribution of the DTI metrics were plotted as histograms and the average and standard deviation of each metric for each sample was calculated. Tests for significance were performed using the students *t*-test (Student, 1908). Significance level was taken to be $p < 0.01$.

3. Results

3.1. Liquid loss and consumer quality results

Liquid loss data for the $-35\text{ }^{\circ}\text{C}$ sample was 2.02% and 5.83% for the $-22\text{ }^{\circ}\text{C}$ sample. For the other samples that have experienced the same storage conditions but were not imaged by MRI, average liquid loss was $2.03 \pm 1.65\%$ for the $-35\text{ }^{\circ}\text{C}$ samples and $6.07 \pm 2.4\%$ for the $-22\text{ }^{\circ}\text{C}$ samples ($p = 0.0004$). On a quality scale of 1 to 5, where 5 is the highest possible quality score, consumer tests on the non-imaged sister samples gave an average score of 4.3 ± 0.48 for the $-35\text{ }^{\circ}\text{C}$ samples and 2.4 ± 0.79 for the $-22\text{ }^{\circ}\text{C}$ samples ($p = 0.0003$). These results indicate clear quality differences between the two frozen samples.

3.2. T_2 -Weighted MRI, DTI and tractography results

Fig. 2 shows an example T_2 -weighted axial image for each sample, the associated FA map for that slice, and the reconstructed tractography in the sagittal view. For the fresh sample, the T_2 image shows smooth, uniform tissue. The $-35\text{ }^{\circ}\text{C}$ sample shows more texture than the fresh

sample, but overall, the tissue appears fairly uniform. The $-22\text{ }^{\circ}\text{C}$ sample shows marbling of bright spots in the tissue, indicative of damage. These results are in line with previous research (Anderssen et al., 2021). The FA maps tend to be more homogeneous for the fresh sample, with significant spatial heterogeneity seen in the $-35\text{ }^{\circ}\text{C}$ sample and to a lesser degree the $-22\text{ }^{\circ}\text{C}$ sample. This is not surprising, as the freezing process will not uniformly affect the sample. Some regions will freeze more quickly than others, leading to variation in the extent that the muscle fiber structure is altered. Although not shown, similar maps are calculated for the RD and AD of the samples. Tractography maps are created to show the most probable distribution and orientation of fibers in the sample based on the spatial distribution of the DTI parameters. Statistical analysis was not performed on the tractography, but visual inspection of the sample shows uniform fiber orientation in the fresh sample. In both the frozen samples, more heterogeneity is visible in the fiber orientation, suggesting disruption during the freezing and thawing process.

Due to the large number of image slices for each sample, it is difficult to evaluate the samples by visual inspection alone. Therefore, the FA, AD, and RD values for all the slices of each sample were converted into histograms, shown Fig. 3. The fresh sample shows uniform FA (0.27 ± 0.07), RD (1.61 ± 0.27) and AD (2.46 ± 0.45). The $-35\text{ }^{\circ}\text{C}$ sample shows an overall shift towards more isotropic diffusion (FA = 0.24 ± 0.08), but there is also increased heterogeneity in the RD (2.12 ± 0.34) and AD (3.09 ± 0.62). The $-22\text{ }^{\circ}\text{C}$ sample shows an even greater shift to more isotropic diffusion (FA = 0.19 ± 0.07 , RD = 2.22 ± 0.34 , AD = 2.96 ± 0.54) but exhibits less heterogeneity than the $-35\text{ }^{\circ}\text{C}$ sample.

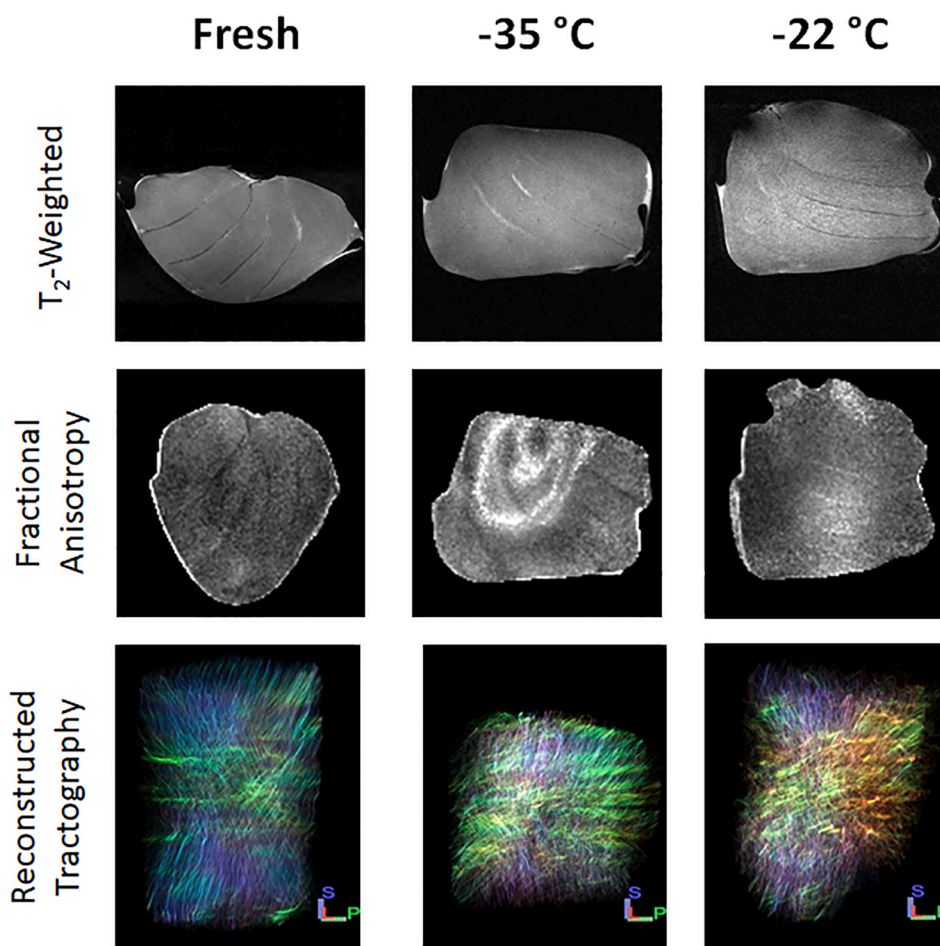


Fig. 2. Imaging results of the three investigated samples under fresh, $-22\text{ }^{\circ}\text{C}$ and $-35\text{ }^{\circ}\text{C}$ conditions, showing in the upper row: a T_2 -weighted axial slice, middle row: associated FA map and bottom: reconstructed sample tractography.

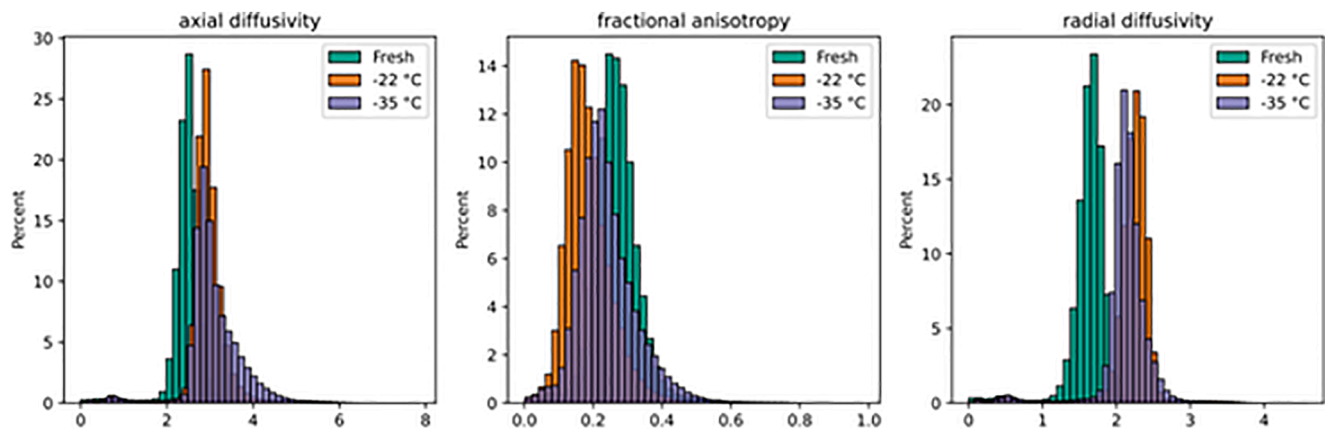


Fig. 3. Histograms for the entire sample for a) axial diffusivity b) fractional anisotropy values c) radial diffusion values.

4. Discussion

4.1. DTI metrics in relation to sample quality

Physical changes in the samples were observed by DTI that are in line with the expected physical changes due to freezing and thawing. The fresh sample showed homogeneity in FA, AD and RD, indicative of uniform tissue. Although no values were found in the food science literature, the values of FA, RD and AD for the fresh sample are similar to what have been observed in healthy skeletal muscle in medical studies (Heemskerk et al., 2010). The tractography indicates that the fresh sample consists of highly parallel muscle fibers.

Frozen storage disrupts this homogeneity. The freezing, frozen storage, and thawing involve both formation of ice crystals and subsequent recrystallizations, something which can tear or burst the cell membrane (Mørkøre and Lilleholt, 2007). Both the samples that had undergone frozen storage showed a shift to lower FA and an increase in the RD, indicative of breakdown in the muscle fiber structure and damage to the cell membrane. Based on previous research (Anderssen et al., 2021; Mulot et al., 2019) and the results of the thaw loss and sensory studies, higher freezing temperatures are associated with greater tissue damage. This is also seen in the DTI metrics, as the $-22\text{ }^{\circ}\text{C}$ sample had a lower mean FA and higher mean RD than the $-35\text{ }^{\circ}\text{C}$ sample. The more damage the muscle fibers experience, the less the structure will restrict diffusion to along the long axis of the cells, allowing water molecules to more freely diffuse in all directions. Although the frozen samples had an overall shift to lower FA, some regions had a shift to higher FA values. While both samples experienced this effect, it was more prominent in the $-35\text{ }^{\circ}\text{C}$ sample, as shown by the bright regions in Fig. 2. These regions also had a decrease in RD and an increase in AD. This indicative of radial shrinkage of the muscle fibers in those locations, another alteration that is known to occur in samples that have been frozen (Sigurgisladottir et al., 2000). As the $-35\text{ }^{\circ}\text{C}$ sister samples were rated as having excellent quality by the consumer test, we speculate that some types of alterations to the muscle structure may have less negative influence on the sensory properties than others. However, given the preliminary nature of this work, further research is necessary on larger sample sets to make any definitive conclusions. Interestingly, these regions of apparent fiber shrinkage were not visible in the T_2 -weighted measurement. This indicates the DTI measurements are able to provide additional insight into food tissue structure that are not apparent by more standard MRI techniques. This conclusion is supported by results from medical studies, where the DTI data was able to detect changes to muscle tissue that the T_2 weighted images were not (Froeling et al., 2014). Visual examination of the tractography of the frozen samples showed a loss of the highly parallel structure seen in the fresh sample, with more prominent disruption in the $-22\text{ }^{\circ}\text{C}$ sample than

the $-35\text{ }^{\circ}\text{C}$ sample.

4.2. Advantages and disadvantages of DTI methodology

The results of this pilot study indicate that DTI could provide a wealth of information not easily obtained by other methods. Further studies are planned to validate the initial findings here more thoroughly. With larger studies combined with more traditional quality metrics such as histology and sensory panels, it may be possible to find correlations between the DTI metrics and meat and seafood quality attributes. Although not investigated in depth in this study, the spatial distribution of the DTI parameters could provide further information on how processing transforms meat and seafood products. The ability to describe the tissue structure in three-dimensions gives the technique a significant advantage over other methods. Drip loss only gives information on tissue damage for a sample as a whole. Texture measurements can only provide information in two dimensions and at a lower resolution than is possible with DTI. The technique also has a significant advantage over other structural evaluation methods like histology in that repeated measurements can be made over time to track changes. The method is also non-invasive, such that the tissue structure can be characterized without influencing it. Histology is well known to be prone to artefacts under sample preparation that alter structure, such as shrinkage, tearing or crushing (Taqi et al., 2018). One of the drawbacks of the DTI technique is the significant acquisition time that is required. However, it is anticipated that this should be possible to improve in the future. A high-quality shim was not possible with the coil available, which is optimized for small animals. A coil optimized for use on samples like meat and fish should enable the use of faster DTI sequences, such as echo planer imaging methods, significantly shortening measurement time. Because the method relies on the diffusion of water, another drawback is that it cannot be used on samples in the frozen state.

5. Conclusions

Diffusion tensor imaging shows promise to provide quantifiable, spatially resolved descriptions of muscle tissue changes due to processing. The properties of fractional anisotropy (FA), radial diffusion (RD) and axial diffusion (AD) help provide information regarding muscle fiber structure and damage. Tissue damage can be identified by decreased FA and increased RD, indicating tearing of the cell membranes of the muscle fibers. Fiber shrinkage appears as an increase in FA and AD, while the RD decreases. Tractography illustrates disruption and breakdown of the fiber structure due to the freezing process. Together, these DTI metrics provide considerably more information for structural characterization of tissue compared to other methods of MRI previously used in food science.

CRediT authorship contribution statement

Kathryn E. Anderssen: Conceptualization, Methodology, Software, Formal analysis, Data curation, Investigation, Resources, Writing – original draft, Funding acquisition. **Mathias Kranz:** Resources, Investigation, Writing – review & editing. **Shaheen Syed:** Software, Formal analysis, Writing – review & editing, Visualization. **Svein Kristian Stormo:** Resources, Methodology, Investigation, Writing – review & editing.

Declaration of Competing Interest

The authors declare that they have no known competing financial interests or personal relationships that could have appeared to influence the work reported in this paper.

Acknowledgements

The authors acknowledge financial support from the Norwegian Research Council through funding grant 294805. The authors thank Angela Mega-Camacho for helpful discussion and the PETcore facility at UiT for the use of the preclinical MRI scanner.

References

- Anderssen, K. E., & McCarney, E. R. (2022). Mechanisms of transverse relaxation of water in muscle tissue. *Food Control*, 132, Article 108373. <https://doi.org/10.1016/j.foodcont.2021.108373>
- Anderssen, K. E., Syed, S., & Stormo, S. K. (2021). Quantification and mapping of tissue damage by freezing in cod by magnetic resonance imaging. *Food Control*, 123, Article 107734. <https://doi.org/10.1016/j.foodcont.2020.107734>
- Aursand, I. G., Veliyulin, E., Bocker, U., Ofstad, R., Rustad, T., & Erikson, U. (2009). Water and salt distribution in Atlantic Salmon (*Salmo salar*) studied by low-field ^1H NMR, ^1H and ^{23}Na MRI and light microscopy: Effects of raw material quality and brine salting. *Journal of Agriculture and Food Chemistry*, 57, 46–54. <https://doi.org/10.1021/jf802158u>
- Basser, P. J. (1995). Inferring microstructural features and the physiological state of tissues from diffusion-weighted images. *NMR in Biomed*, 8, 333–344. <https://doi.org/10.1002/nbm.1940080707>
- Callaghan, P. T. (2011). *Translational dynamics and magnetic resonance: principles of pulsed gradient spin echo NMR*. Oxford University Press.
- Erikson, U., Veliyulin, E., Singstad, T. E., & Aursand, I. G. (2004). Salting and desalting of fresh and frozen-thawed cod (*Gadus morhua*) fillets: A comparative study using ^{23}Na NMR, ^{23}Na MRI, Low-field ^1H NMR, and physicochemical analytical methods. *Journal of Food Science*, 69(3), 107–114. <https://doi.org/10.1111/j.1365-2621.2004.tb13362.x>
- Froeling, M., Oudeman, J., Strijkers, G. J., Maas, M., Drost, M. R., Nicolay, K., & Nederveen, A. J. (2014). Muscle changes detected with diffusion-tensor imaging after long distance running. *Radio*, 274, 548–562. <https://doi.org/10.1148/radiol.14140702>
- Gudjonsdottir, M., Traore, A., Jonsson, A., Karlsdottir, M. G., & Arason, S. (2015). The effects of pre-salting methods on salt and water distribution of heavily salted cod, as analyzed by ^1H and ^{23}Na MRI, ^{23}Na NMR, low-field NMR and physicochemical analysis. *Food Chemistry*, 188, 664–672. <https://doi.org/10.1016/j.foodchem.2015.05.060>
- Heemskerck, A. M., Sinha, T. K., Wilson, K. J., Ding, Z., & Damon, B. M. (2010). Repeatability of DTI-based skeletal muscle fiber tracking. *NMR in Biomedicine*, 23, 294–303. <https://doi.org/10.1002/nbm.1463>
- Howell, N., Shavila, Y., Grootveld, M., & Williams, S. (1996). High-Resolution NMR and magnetic resonance imaging (MRI) studies on fresh and frozen cod (*Gadus morhua*) and haddock (*Melanogrammus aeglefinus*). *Journal of the Science of Food and Agriculture*, 72(1), 49–56. [https://doi.org/10.1002/\(SICI\)1097-0010\(199609\)72:1<49::AID-JSFA621>3.0.CO;2-H](https://doi.org/10.1002/(SICI)1097-0010(199609)72:1<49::AID-JSFA621>3.0.CO;2-H)
- Hyldig, G., & Green-Petersen, D. M. B. (2008). Quality index method - an objective tool for determination of sensory quality. *Journal of Aquatic Food Product Technology*, 13, 71–80. https://doi.org/10.1300/J030v13n04_06
- Johnston, I. A., Alderson, R., Sandham, C., & Dingwall, A. (2000). Muscle fibre density in relation to the colour and texture of smoked Atlantic salmon (*Salmo salar* L.). *Aquaculture*, 189, 335–349. [https://doi.org/10.1016/S0044-8486\(00\)00373-2](https://doi.org/10.1016/S0044-8486(00)00373-2)
- Kalab, M., Allan-Wojatas, P., & Miller, S. (1995). Microscopy and other imaging techniques in food structure analysis. *Trends in Food Science and Technology*, 6, 177–186. [https://doi.org/10.1016/S0924-2244\(00\)89052-4](https://doi.org/10.1016/S0924-2244(00)89052-4)
- Le Bihan, D., Mangin, J. F., Poupon, C., Clark, C. A., Pappata, S., Molko, N., & Chabriat, H. (2001). Diffusion tensor imaging: Concepts and applications. *Journal of Magnetic Resonance Imaging*, 14, 534–546. <https://doi.org/10.1002/jmri.1076>
- Mulot, V., Fatou, Toutie, N., Benkhalifa, H., Pathier, D., & Flick, D. (2019). Investigating the effect of freezing operating conditions on microstructure of frozen minced beef using an innovative X-ray micro-computed tomography method. *Journal of Food Engineering*, 262, 13–21. <https://doi.org/10.1016/j.jfoodeng.2019.05.014>
- Mørkøre, T., & Lilleholt, R. (2007). Impact of freezing temperature on quality of farmed Atlantic Cod (*Gadus morhua* L.). *Journal of Texture Studies*, 34(4), 457–472. <https://doi.org/10.1111/j.1745-4603.2007.00108.x>
- Nott, K. P., Evans, S. D., & Hall, L. D. (1999). The Effect of freeze-thawing on the magnetic resonance imaging parameters of cod and mackerel. *LWT Food Science and Technology*, 32(5), 261–268. <https://doi.org/10.1006/food.1999.0549>
- Sigurgisladottir, S., Ingvarsdottir, H., Torrisen, O. J., Cardinal, M., & Hafsteinsson, H. (2000). Effects of freezing/thawing on the microstructure and the texture of smoked Atlantic salmon (*Salmo salar*). *Food Research International*, 33, 857–865. [https://doi.org/10.1016/S0963-9969\(00\)00105-8](https://doi.org/10.1016/S0963-9969(00)00105-8)
- Student (1908), The Probable Error of a Mean, *Biometrika*, 6, 1-25.
- Taqi, S. A., Sami, S. A., Sami, L. B., & Zaki, S. A. (2018). A review of artifacts in histopathology. *Journal of Oral and Maxillofacial Pathology*, 22, 279. https://doi.org/10.4103/jomfp.JOMFP_125_15
- Tolstorebrov, I., Eikevik, T. M., & Bantle, M. (2016). Effect of low and ultra-low temperature applications during freezing and frozen storage on quality parameters for fish. *International Journal of Refrigeration*, 63, 37–47. <https://doi.org/10.1016/j.ijrefrig.2015.11.003>
- Vestergaard, C., Risum, J., & Adler-Nissen, J. (2005). ^{23}Na -MRI quantification of sodium mobility in pork during brine curing. *Meat Science*, 69, 663–672. <https://doi.org/10.1016/j.meatsci.2004.11.001>
- Yeh, F.-C. (2021, May 15). DSI Studio (Version 2021 May). Zenodo. <http://doi.org/10.5281/zenodo.4764264>.
- Yeh, F.-C., Verstynen, T. D., Wang, Y., Fernandez-Miranda, J. C., & Tseng, W.-Y.-I. (2013). Deterministic diffusion fiber tracking improved by quantitative anisotropy. *PLoS One*. <https://doi.org/10.1371/journal.pone.0080713>